

Supplementary information

Unusual variability of isomers in copper(II) complexes with 1,8-bis(2-hydroxybenzyl)-cyclam

Milan Mařar,^a Jan Faltejsek,^{a,b} Hana Buřková,^{b,c} Lucie Koláčná,^d Adam Jaroř,^b Jan Kotek,^a Michal Straka,^b Vojtěch Kubíček^{a*} and Jiří Ludvík^d

^a Department of Inorganic Chemistry, Faculty of Science, Charles University, Hlavova 8, 128 40 Prague 2, Czech Republic. e-mail: kubicek@natur.cuni.cz

^b Czech Academy of Sciences, Institute of Organic Chemistry and Biochemistry, Flemingovo náměstí 542/2, 160 00 Prague 6, Czech Republic

^c Department of Physical and Macromolecular Chemistry, Faculty of Science, Charles University, Hlavova 8, 128 40 Prague 2, Czech Republic

^d Czech Academy of Sciences, J. Heyrovsky Institute of Physical Chemistry, Dolejškova 2155/3, 182 23 Prague 8, Czech Republic

Table of content

UV-VIS study	4
Figure S1. UV-VIS spectra and absorbance in the maximum of the absorption band as function of time measured in the course of mutual interconversion of the <i>cis</i> - I and <i>cis</i> - V isomers	4
Figure S2. UV-VIS spectra and absorbance in the maximum of the absorption band as function of time measured in the course of <i>trans</i> - III isomer formation	5
X-ray diffraction study	6
Table S1. Hydrogen bonds' geometries in the solid-state structure of H ₂ L	7
Table S2. Hydrogen bonds' geometries in the solid-state structure of (H ₄ L)(ClO ₄) ₂	7
Figure S3. Solid-state structure of compound III^A : <i>trans</i> -[Cu(L)]·2CH ₃ OH	8
Figure S4. Solid-state structure of compound III^B : <i>trans</i> -[Cu(L)]·2H ₂ O	8
Figure S5. Solid-state structure of compound III^C : <i>trans</i> -[Cu(H ₂ L)]Cl ₂	9
Figure S6. Solid-state structure of compound III^D : <i>trans</i> -[Cu(HL)]Cl·H ₂ O	9
Figure S7. Solid-state structure of compound III^E : <i>trans</i> -[Cu(H ₂ L)](CF ₃ CO ₂) ₂	10

Figure S8. Solid-state structure of compound III^F : <i>trans</i> -[Cu(H ₂ L)][Cu(H ₂ L)(SO ₄) ₂] \cdot 6CH ₃ OH	10
Figure S9. Solid-state structure of compound V^A : <i>cis</i> -[Cu(HL)] ₂ SO ₄ \cdot 6CH ₃ OH	11
Figure S10. Solid-state structure of compound V^B : <i>cis</i> -[Cu(HL)](CF ₃ CO ₂)	11
Table S3. Selected bond lengths and angles in hexacoordinated complexes	12
Table S4. Selected bond lengths and angles in pentacoordinated complexes	13
Table S5. Hydrogen bonds' geometries in the solid-state structure of <i>trans</i> -[Cu(L)] \cdot 2CH ₃ OH (III^A)	14
Table S6. Hydrogen bonds' geometries in the solid-state structure of <i>trans</i> -[Cu(L)] \cdot 2H ₂ O (III^B)	14
Table S7. Hydrogen bonds' geometries in the solid-state structure of <i>trans</i> -[Cu(H ₂ L)]Cl ₂ (III^C)	14
Table S8. Hydrogen bonds' geometries in the solid-state structure of <i>trans</i> -[Cu(HL)]Cl \cdot H ₂ O (III^D)	14
Table S9. Hydrogen bonds' geometries in the solid-state structure of <i>trans</i> -[Cu(H ₂ L)](CF ₃ CO ₂) ₂ (III^E)	15
Table S10. Hydrogen bonds' geometries in the solid-state structure of <i>trans</i> -[Cu(H ₂ L)][Cu(H ₂ L)(SO ₄) ₂] \cdot 6CH ₃ OH (III^F)	15
Table S11. Selected hydrogen bonds' geometries in the solid-state structure of <i>cis</i> -[Cu(HL)] ₂ SO ₄ \cdot 6CH ₃ OH (V^A)	16
Table S12. Hydrogen bonds' geometries in the solid-state structure of <i>cis</i> -[Cu(HL)](CF ₃ CO ₂) (V^B)	16
Table S13. Experimental data of crystal structures	17
Theoretical calculations	18
Relative energies of isomers in the model using a purely implicit solvent	18
Table S14. Predicted relative electronic energies of the lowest minima of isomers relative to the isomer III in the purely implicit solvent	20
Table S15. Predicted relative electronic energies of the lowest minima of isomers relative to the isomer III in the model with two explicit water molecules included	20
Table S16. Calculated protonation constants p <i>K</i> _A of individual isomers in the models with the purely implicit solvent and with the two explicit water molecules included	21
Table S17. Predicted interatomic O-O/M distances and calculated delocalization indices for selected bonds and isomers	21
Figure S11. Calculated optimized structures of deprotonated isomers	22

Figure S12. Calculated optimized structures of monoprotinated isomers	22
Figure S13. Calculated optimized structures of diprotinated isomers	23
Figure S14. Optimized structures of deprotonated isomers calculated in the model with the two explicit water molecules included	23
Figure S15. Optimized structures of diprotinated isomers calculated in the model with the two explicit water molecules included	24
Table S18. Calculated reduction potentials of deprotonated, monoprotinated and diprotinated isomers based on the model with purely implicit solvent or with two explicit water molecules	25
Table S19. Predicted interatomic M-O/N distances in the lowest conformers in the model with two explicit water molecules	25
Figure S16. Calculated optimized structures of the <i>cis-I</i> isomer in all studied protonation states with two explicit water molecules	26
Figure S17. Calculated optimized structures of the <i>cis-V</i> isomer in all studied protonation states with two explicit water molecules	26
Figure S18. Energy scan as function of Cu–O distance in the monoprotinated isomer <i>cis-V</i>	27
Figure S19. Energy scan as function of Cu–O distance in the deprotonated isomer <i>cis-I</i>	27
Table S20. Predicted relative total free Gibbs energies from the COSMO-RS protocol of the lowest [Cu(L)] conformers relative to the isomer <i>trans-III</i>	28

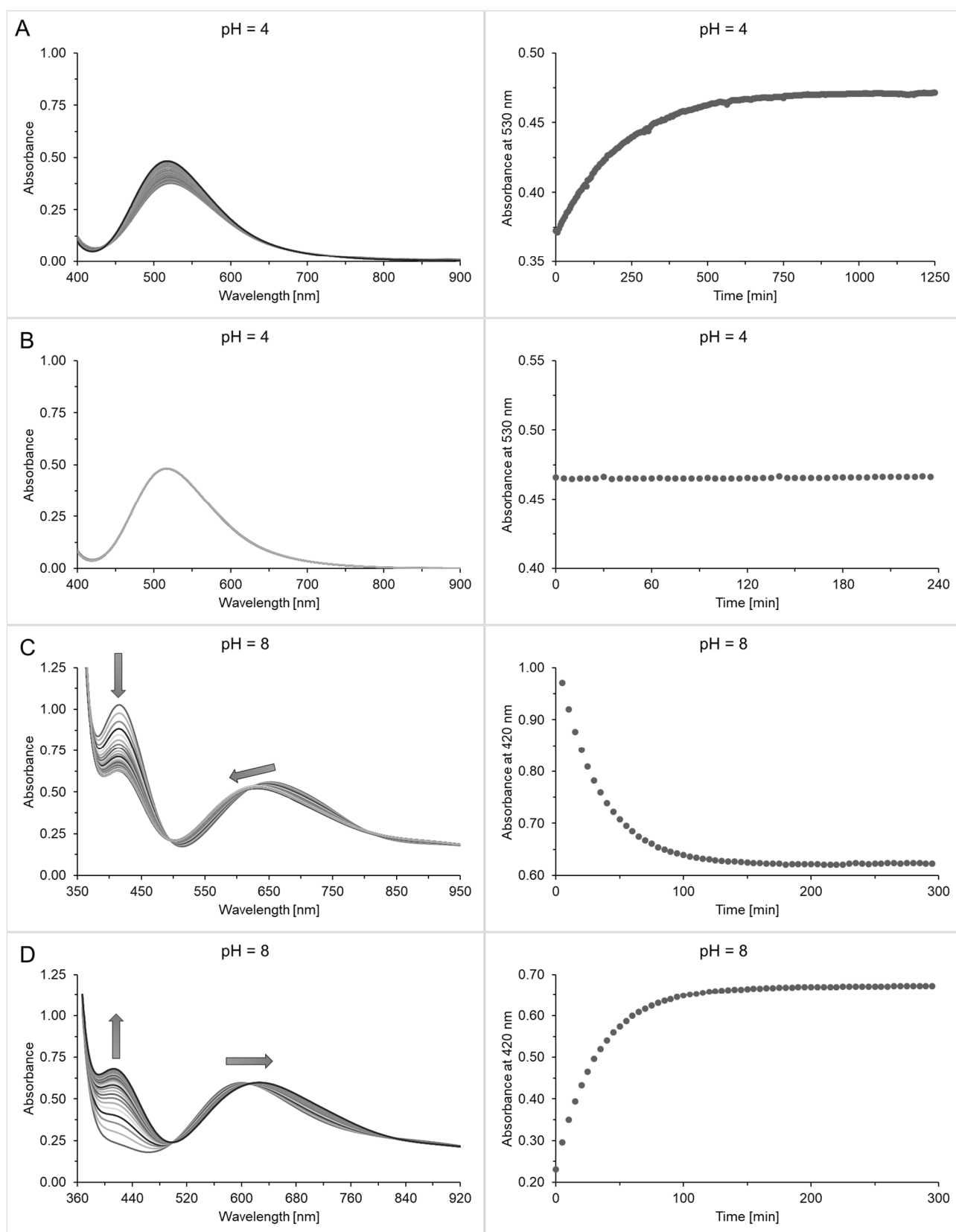


Figure S1. UV-VIS spectra (left) and absorbance in the maximum of the absorption band as function of time(right) measured in the course of mutual interconversion of the *cis*-I and *cis*-V isomers at pH 4 (A and B) or 8 (C and D) (25 °C, $c_{\text{CuL}} = 4 \text{ mM}$). The process started with *cis*-V (plots A and C) or *cis*-I isomer (plots B and D). All spectra in the plot B are identical, as no isomerization proceeds.

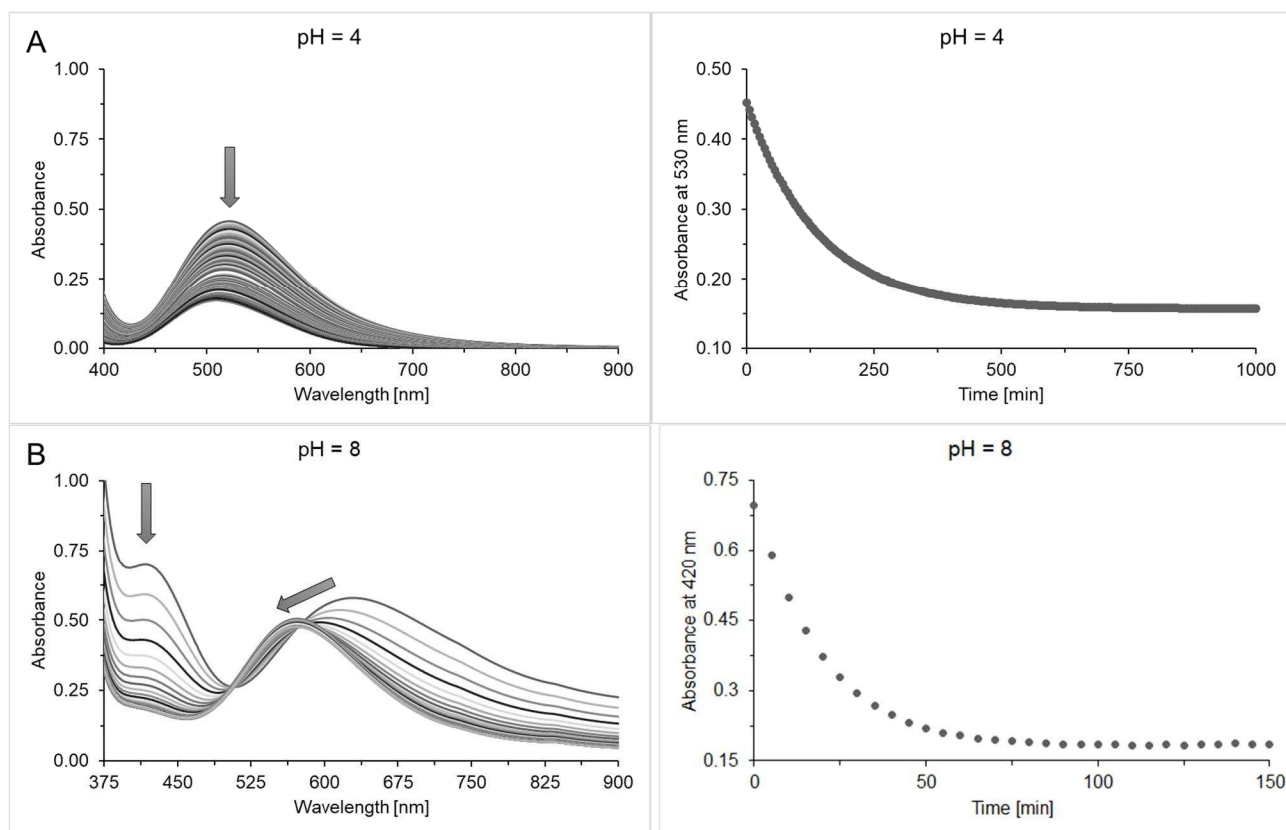


Figure S2. UV-VIS spectra (left) and absorbance in the maximum of the absorption band as function of time (right) measured in the course of *trans*-**III** isomer formation from the equilibrium mixture of the *cis*-**I** and *cis*-**V** at pH 4 (A) or 8 (B) (90 °C, $c_{\text{CuL}} = 4 \text{ mM}$).

X-ray diffraction study

The ligand molecules found in the crystal structures of H₂L and (H₄L)(ClO₄)₂ are centrosymmetric. In the electroneutral molecule of H₂L found in its crystal structure, the phenol groups are protonated and the macrocycle adopts ‘common’ conformation¹ of the cyclam ring typical for cyclam derivatives with non-charged macrocycle amino-groups, whereas the macrocyclic part in the diprotonated molecule (H₄L)²⁺ found in the crystal structure of (H₄L)(ClO₄)₂ adopts conformation (3,4,3,4)-B, which is the most frequent conformation of cyclams with protonated macrocycle amines.^{1,2}

In the crystal structure of *trans*-[Cu(L)]·2CH₃OH (**III^A**), two centrosymmetric halves of the complex molecules form the structurally independent unit together with two methanol molecules. In the crystal structures of *trans*-[Cu(L)]·2H₂O (**III^B**), *trans*-[Cu(H₂L)]Cl₂ (**III^C**) and *trans*-[Cu(H₂L)][Cu(H₂L)(SO₄)₂]·6CH₃OH (**III^F**), the independent unit corresponds to one half of the formula unit, and all the complex molecules possess centres of symmetry. In the crystal structure of *trans*-[Cu(HL)]Cl·H₂O (**III^D**), the independent unit corresponds to one half of the formula unit and the complex molecule again possess the symmetry centre. The chloride anion and water molecules of crystallization were found in very close positions, so the occupancies of both fragments were defined to be 50% to achieve the electroneutrality of the compound. In the crystal structure of *trans*-[Cu(H₂L)](CF₃CO₂)₂ (**III^E**), the independent unit corresponds to one half of the formula unit and the complex molecule possess the symmetry centre as in all other structures of the *trans*-**III** isomer. The fluorine atoms of trifluoroacetate anion were found disordered – the trifluoromethyl group was best refined staggered in three positions with relative occupancies 58:29:13%. In the crystal structure of *cis*-[Cu(HL)]₂SO₄·6CH₃OH (**V^A**), the structurally independent motif consists from the formula unit. Two independent complex molecules are interconnected through sulphate anion disordered in two positions *via* hydrogen bonds from non-coordinated protonated phenol moieties. Five of six methanol molecules of crystallization were best refined each disordered in two positions, with the hydrogen atoms of the O–H groups fixed in the original positions from the electron density map using $U_{\text{eq}}(\text{H}) = 1.5 U_{\text{eq}}(\text{O})$ as the free refinement led to unrealistic bond lengths or thermal parameters. In the crystal structure of *cis*-[Cu(HL)](CF₃CO₂) (**V^B**), the structurally independent unit corresponds to the formula unit. The trifluoroacetate anion was best refined as disordered over two positions sharing the carboxylate carbon atom.

¹ P. Hermann, J. Kotek and V. Kubíček, Ten-Membered Rings or Lager with One or More Nitrogen Atoms. In: D. Black, J. Cossy, Ch. V. Stevens, Comprehensive Heterocyclic Chemistry IV., 2022, **14**, 591. Oxford: Elsevier.

² M. Meyer, V. Dahaoui-Gindrey, C. Lecomte and R. Guilard, *Coord. Chem. Rev.*, 1998, **178–180**, 1313.

Table S1. Hydrogen bonds' geometries in the solid-state structure of H₂L [\AA and $^\circ$].

D-H \cdots A	$d(\text{D-H})$	$d(\text{H}\cdots\text{A})$	$\angle(\text{DHA})$	$d(\text{D}\cdots\text{A})$	A
N4-H41	0.91(1)	2.23(1)	135(1)	2.950(1)	N1 $[-x+1, -y+1, -z+1]$
N4-H41	0.91(1)	2.68(1)	130(1)	3.336(2)	N4 $[-x+1, -y+1, -z+1]$
O10-H101	0.94(2)	2.58(2)	125(1)	3.210(1)	N1
O10-H101	0.94(2)	1.79(2)	158(2)	2.686(1)	N4

Table S2. Hydrogen bonds' geometries in the solid-state structure of (H₄L)(ClO₄)₂ [\AA and $^\circ$].

D-H \cdots A	$d(\text{D-H})$	$d(\text{H}\cdots\text{A})$	$\angle(\text{DHA})$	$d(\text{D}\cdots\text{A})$	A
N4-H41	0.85(2)	2.03(2)	164(2)	2.862(1)	O10
N4-H42	0.91(2)	2.32(2)	139(1)	3.062(2)	O2P $[x, -y+3/2, z+1/2]$
N4-H42	0.91(2)	2.43(2)	132(1)	3.113(1)	O4P
O10-H101	0.83(2)	2.00(2)	161(2)	2.793(1)	O1P

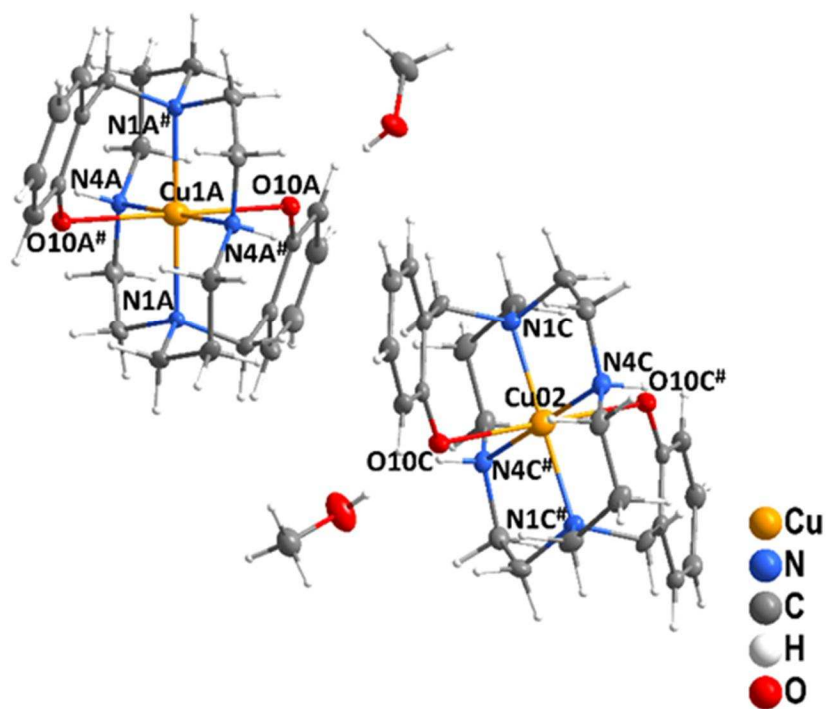


Figure S3. Solid-state structure of compound **III^A**: *trans*-[Cu(L)]·2CH₃OH.

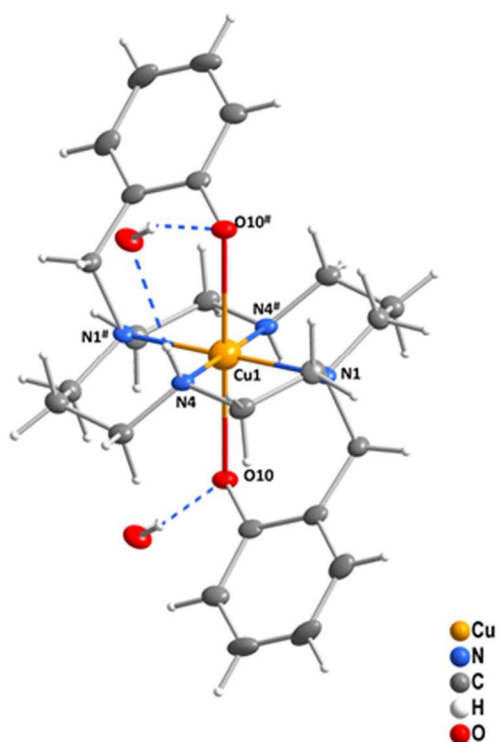


Figure S4. Solid-state structure of compound **III^B**: *trans*-[Cu(L)]·2H₂O.

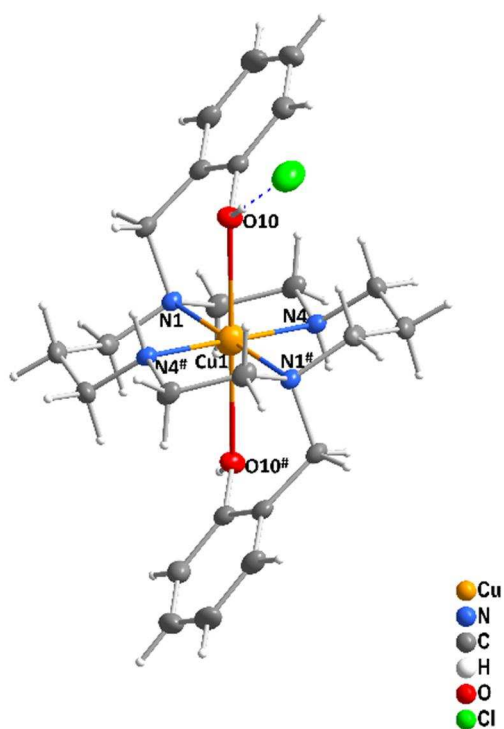


Figure S5. Solid-state structure of compound **III^C**: *trans*-[Cu(H₂L)]Cl₂.

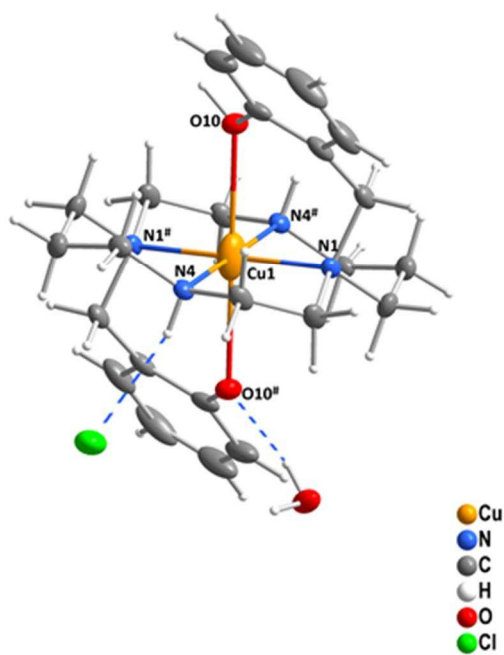


Figure S6. Solid-state structure of compound **III^D**: *trans*-[Cu(HL)]Cl·H₂O.

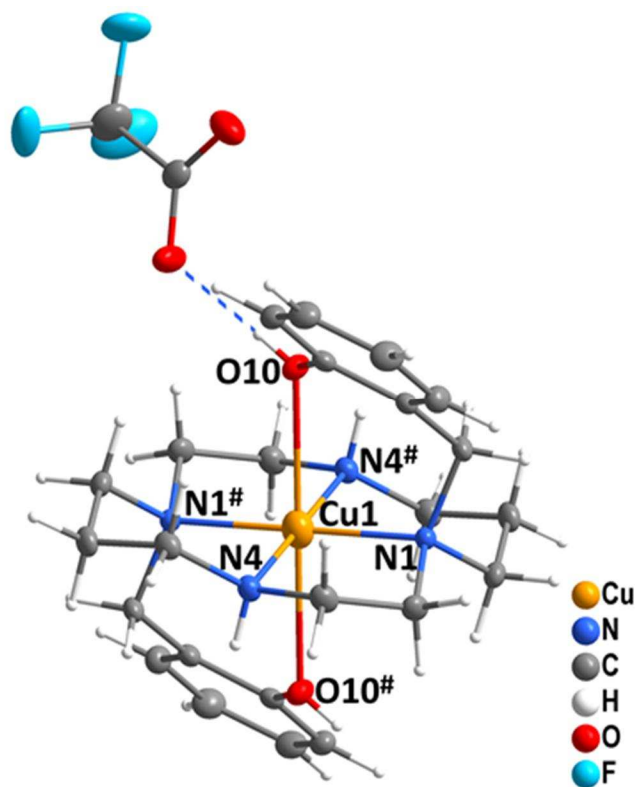


Figure S7. Solid-state structure of compound **III^E**: $trans$ -[Cu(H₂L)](CF₃CO₂)₂.

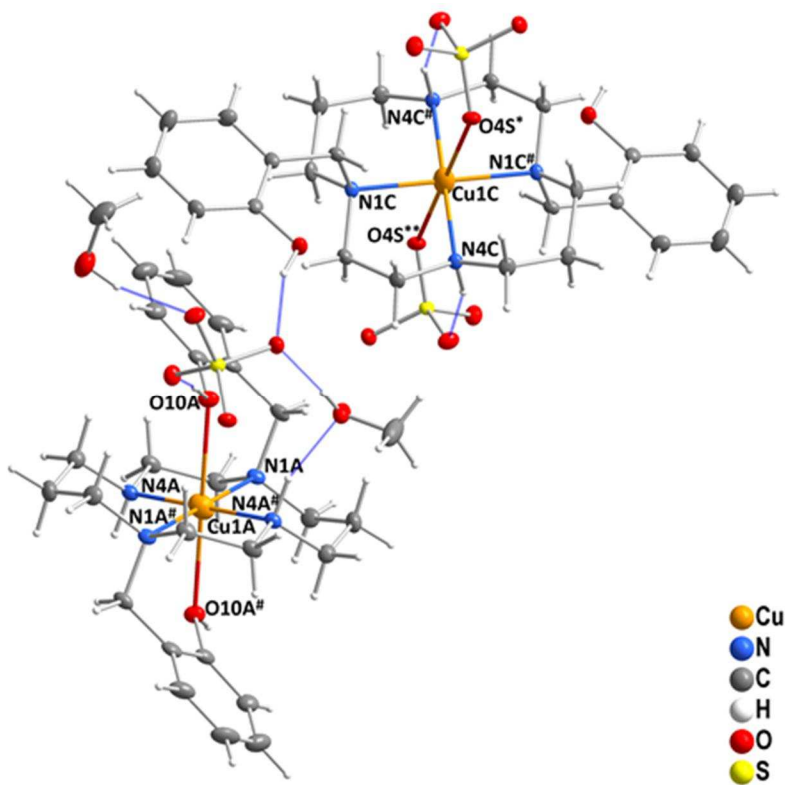


Figure S8. Solid-state structure of compound **III^F**: $trans$ -[Cu(H₂L)][Cu(H₂L)(SO₄)₂]·6CH₃OH.

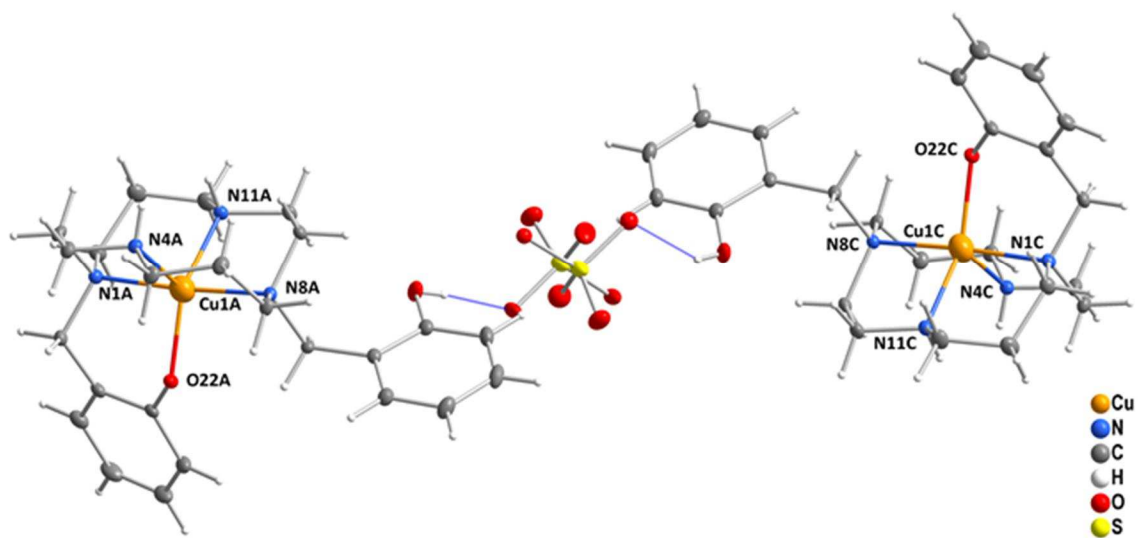


Figure S9. Solid-state structure of compound **V^A**: *cis*-[Cu(HL)]₂SO₄·6CH₃OH.

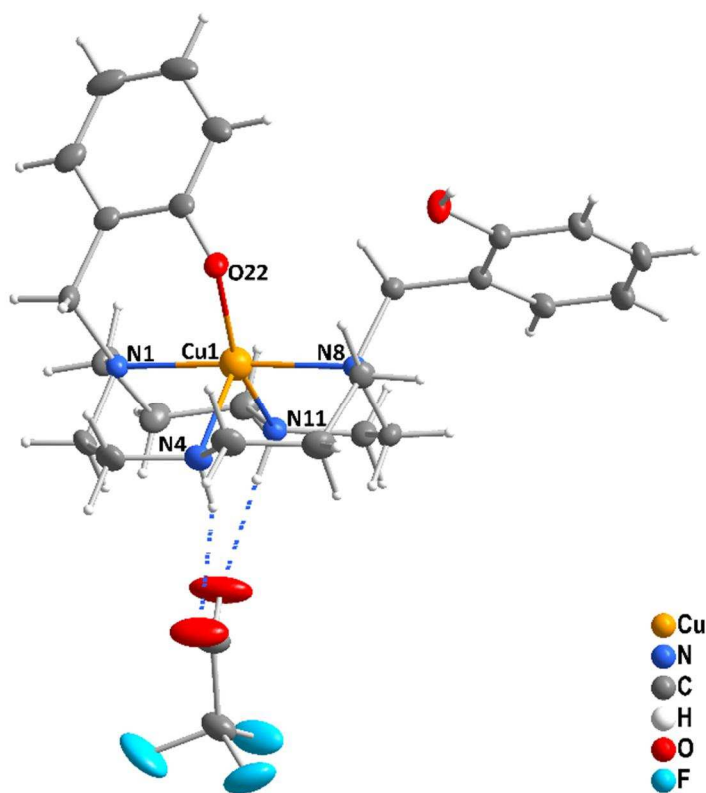


Figure S10. Solid-state structure of compound **V^B**: *cis*-[Cu(HL)](CF₃CO₂).

Table S3. Selected bond lengths [\AA] and angles [$^\circ$] in hexacoordinated complexes.

	<i>trans</i> -[Cu(L)] ·2CH ₃ OH (III^A)		<i>trans</i> - [Cu(L)]· 2H ₂ O (III^B)	<i>trans</i> - [Cu(H ₂ L)]Cl ₂ (III^C)	<i>trans</i> - [Cu(HL)]Cl· H ₂ O (III^D)	<i>trans</i> - [Cu(H ₂ L)] (CF ₃ CO ₂) ₂ (III^E)	<i>trans</i> - [Cu(H ₂ L)][Cu(H ₂ L)(SO ₄) ₂] ·6CH ₃ OH (III^F)		<i>trans</i> -[Cu(H ₂ L)] (CH ₃ CO ₂) ₂ · 2H ₂ O reported in ref. 1
	<i>mol. A</i>	<i>mol. B</i>					<i>mol. A</i>	<i>mol. B</i>	
Cu–N1	2.054(1)	2.042(1)	2.059(3)	2.053(1)	2.053(1)	2.064(1)	2.052(2)	2.081(2)	2.046(2)
Cu–N4	2.018(1)	2.046(1)	2.027(3)	2.012(1)	2.018(1)	2.007(1)	2.007(2)	1.996(2)	2.013(2)
Cu–O10	2.405(1)	2.369(1)	2.462(2)	2.526(1)	2.491(1)	2.521(1)	2.524(2)	2.681(1)	2.652(2)
N1–Cu–N1 ^{#1}	180	180	180	180	180	180	180	180	180
N4–Cu–N4 ^{#1}	180	180	180	180	180	180	180	180	180
N4–Cu–N1 ^{#1}	92.80(5)	93.36(5)	93.76(9)	93.18(6)	93.46(4)	93.15(5)	92.89(7)	93.49(6)	93.02(8)
N4–Cu–N1	87.20(5)	86.64(5)	86.24(9)	86.82(6)	86.54(4)	86.85(5)	87.11(7)	86.51(6)	86.98(8)
N1–Cu–O10	88.73(4)	97.26(5)	87.81(9)	87.05(5)	87.55(4)	86.02(4)	86.26(6)	94.61(5)	94.61(7)
N4–Cu–O10	97.67(4)	89.64(4)	94.26(8)	94.99(5)	95.11(4)	96.92(4)	97.08(6)	92.73(6)	91.16(7)
N1–Cu–O10 ^{#1}	91.27(4)	90.36(4)	92.19(9)	92.95(5)	92.45(4)	93.98(4)	93.74(6)	85.39(5)	85.39(7)
N4–Cu–O10 ^{#1}	82.33(4)	82.74(5)	85.74(8)	85.01(5)	84.89(4)	83.08(4)	82.92(6)	87.27(6)	88.84(7)

#1: centrosymmetry-related atom; the centre of symmetry is located in the copper ion position

Ref. 1: H. Luo, R. D. Rogers and M. W. Brechbiel, *Can J Chem*, 2001, **79**, 1105–1109.

Table S4. Selected bond lengths [\AA] and angles [$^\circ$] in pentacoordinated complexes.

	<i>cis</i> -[Cu(HL)] ₂ SO ₄ ·6CH ₃ OH (V^A)		<i>cis</i> -[Cu(HL)](CF ₃ CO ₂) (V^B)
	<i>var. A</i>	<i>var. B</i>	
Cu–N1	2.088(2)	2.080(2)	2.086(1)
Cu–N4	2.176(2)	2.181(2)	2.197(1)
Cu–N8	2.119(2)	2.092(2)	2.073(1)
Cu–N11	2.048(2)	2.054(2)	2.020(1)
Cu–O22	1.972(2)	1.974(2)	1.963(1)
N1–Cu–N4	84.25(9)	84.34(9)	85.08(5)
N1–Cu–N8	175.72(8)	176.08(9)	177.53(5)
N1–Cu–N11	92.47(9)	92.15(9)	92.92(5)
N4–Cu–N8	93.39(9)	93.79(9)	93.49(5)
N4–Cu–N11	101.46(9)	100.28(9)	100.48(5)
N8–Cu–N11	84.49(9)	84.78(9)	85.35(5)
N1–Cu–O22	92.77(8)	93.28(9)	91.31(4)
N4–Cu–O22	107.74(9)	106.95(9)	102.91(5)
N8–Cu–O22	91.35(8)	90.56(8)	90.97(4)
N11–Cu–O22	150.71(9)	152.62(9)	156.50(5)

Table S5. Hydrogen bonds' geometries in the solid-state structure of *trans*-[Cu(L)]·2CH₃OH (**III^A**) [\AA and $^\circ$].

D–H \cdots A	<i>d</i> (D–H)	<i>d</i> (H \cdots A)	\angle (DHA)	<i>d</i> (D \cdots A)	A
N4A–H4A	0.88(2)	2.45(2)	115(1)	2.926(2)	O10A [– <i>x</i> +1, – <i>y</i> +1, – <i>z</i> +2]
N4C–H4C	0.88(2)	2.48(2)	112(2)	2.928(2)	O10C [– <i>x</i> +1, – <i>y</i> , – <i>z</i> +1]
N4C–H4C	0.88(2)	2.44(2)	151(2)	3.241(2)	O2M [– <i>x</i> +1, – <i>y</i> , – <i>z</i> +1]
O1M–H1MO	0.74(2)	1.92(3)	171(3)	2.654(2)	O10A
O2M–H2MO	0.74(3)	1.89(3)	168(3)	2.622(2)	O10C

Table S6. Hydrogen bonds' geometries in the solid-state structure of *trans*-[Cu(L)]·2H₂O (**III^B**) [\AA and $^\circ$].

D–H \cdots A	<i>d</i> (D–H)	<i>d</i> (H \cdots A)	\angle (DHA)	<i>d</i> (D \cdots A)	A
N4–H41	0.80(4)	2.26(5)	176(4)	3.055(4)	O1W [<i>x</i> , <i>y</i> –1, <i>z</i>]
O1W–H11W	0.73(6)	2.03(6)	170(6)	2.749(3)	O10
O1W–H12W	0.76(5)	2.04(5)	156(5)	2.759(4)	O10 [– <i>x</i> +1, – <i>y</i> +2, – <i>z</i> +1]

Table S7. Hydrogen bonds' geometries in the solid-state structure of *trans*-[Cu(H₂L)]Cl₂ (**III^C**) [\AA and $^\circ$].

D–H \cdots A	<i>d</i> (D–H)	<i>d</i> (H \cdots A)	\angle (DHA)	<i>d</i> (D \cdots A)	A
N4–H41	0.88(2)	2.62(2)	114(2)	3.089(2)	O10 [– <i>x</i> +1, – <i>y</i> +1, – <i>z</i> +1]
N4–H41	0.88(2)	2.44(2)	158(2)	3.272(2)	Cl1 [<i>x</i> , <i>y</i> +1, <i>z</i>]
O10–H101	0.75(3)	2.25(3)	175(2)	2.992(1)	Cl1

Table S8. Hydrogen bonds' geometries in the solid-state structure of *trans*-[Cu(HL)]Cl·H₂O (**III^D**) [\AA and $^\circ$].

D–H \cdots A	<i>d</i> (D–H)	<i>d</i> (H \cdots A)	\angle (DHA)	<i>d</i> (D \cdots A)	A
N4–H41	0.87(2)	2.61(2)	113(1)	3.063(1)	O10 [– <i>x</i> +1, – <i>y</i> +1, – <i>z</i> +1]
N4–H41	0.87(2)	2.41(2)	159(2)	3.241(1)	Cl1 [<i>x</i> , <i>y</i> +1, <i>z</i>]
N4–H41	0.87(2)	2.19(2)	177(2)	3.054(3)	O1W [<i>x</i> , <i>y</i> +1, <i>z</i>]
O10–H101	0.91 ^a	2.07 ^a	170 ^a	2.976(1)	Cl1
O1W–H1W	0.88 ^a	1.87 ^a	168 ^a	2.742(3)	O10
O1W–H2W	0.85 ^a	1.94 ^a	165 ^a	2.768(3)	O10 [– <i>x</i> +1, – <i>y</i> , – <i>z</i> +1]

^a No ESDs are given for hydrogen atoms fixed in theoretical positions.

Table S9. Hydrogen bonds' geometries in the solid-state structure of *trans*-[Cu(H₂L)](CF₃CO₂)₂ (**III^E**) [Å and °].

D-H...A	<i>d</i> (D-H)	<i>d</i> (H...A)	<(DHA)	<i>d</i> (D...A)	A
N4-H41	0.89 ^a	2.23 ^a	139 ^a	2.952(2)	O2A [-x+1, y+1/2, -z+3/2]
O10-H101	0.74(3)	1.82(3)	172(3)	2.550(2)	O1A

^a No ESDs are given for hydrogen atoms fixed in theoretical positions.

Table S10. Hydrogen bonds' geometries in the solid-state structure of *trans*-[Cu(H₂L)][Cu(H₂L)(SO₄)₂].6CH₃OH (**III^F**) [Å and °].

D-H...A	<i>d</i> (D-H)	<i>d</i> (H...A)	<(DHA)	<i>d</i> (D...A)	A
N4A-H4A	1.00 ^a	1.92 ^a	161 ^a	2.886(2)	O1M [-x+1, -y+1, -z+1]
N4C-H4C	1.00 ^a	1.87 ^a	159 ^a	2.828(2)	O3S [-x+1, y+1/2, -z+1/2]
O10A-H10A	0.82(3)	1.75(3)	169(3)	2.560(2)	O1S
O10C-H10C	0.84(3)	1.82(4)	160(3)	2.626(2)	O2S
O1M-H1MO	0.75(3)	1.97(3)	174(3)	2.715(2)	O2S
O2M-H2MO	0.85(4)	1.86(4)	160(3)	2.683(2)	O3S
O3M-H3MO	0.93(4)	1.89(4)	173(3)	2.811(2)	O2M

^a No ESDs are given for hydrogen atoms fixed in theoretical positions.

Table S11. Selected hydrogen bonds' geometries in the solid-state structure of *cis*-[Cu(HL)]₂SO₄·6CH₃OH (**V^A**) [Å and °].

D–H⋯A	<i>d</i> (D–H)	<i>d</i> (H⋯A)	<(DHA)	<i>d</i> (D⋯A)	A
N4A–H4A	0.84(4)	2.27(4)	145(3)	3.003(3)	O1S ^a [x–1, y, z]
N4A–H4A	0.84(4)	2.17(5)	161(3)	2.98(3)	O4T ^a [x–1, y, z]
N11A–H11A	0.87(4)	1.98(4)	165(4)	2.831(3)	O2S ^a [x–1, y, z]
N11A–H11A	0.87(4)	2.29(5)	158(4)	3.12(3)	O3T ^a [x–1, y, z]
O32A–H32A	0.87(5)	1.76(4)	170(4)	2.624(3)	O1S ^a
O32A–H32A	0.87(5)	2.06(5)	137(4)	2.77(2)	O1T ^a
N4C–H4C	0.82(4)	2.37(4)	158(3)	3.144(4)	O4S ^a [x+1, y, z]
N4C–H4C	0.82(4)	2.28(4)	142(3)	2.97(2)	O2T ^a [x+1, y, z]
N11C–H11C	0.83(4)	2.15(4)	155(3)	2.959(4)	O3S ^a [x+1, y, z]
N11C–H11C	0.83(4)	1.93(4)	170(4)	2.71(2)	O1T ^a [x+1, y, z]
O32C–H32C	0.87 ^b	1.87 ^b	154 ^b	2.675(3)	O2S ^a
O32C–H32C	0.87 ^b	1.92 ^b	145 ^b	2.67(2)	O2T ^a

^a Oxygen atoms of disordered sulphate anion: label “S” was used for the more abundant position (90%), label “T” for the less abundant position (10%). ^b No ESDs are given for hydrogen atoms fixed in theoretical positions.

Table S12. Hydrogen bonds' geometries in the solid-state structure of *cis*-[Cu(HL)](CF₃CO₂) (**V^B**) [Å and °].

D–H⋯A	<i>d</i> (D–H)	<i>d</i> (H⋯A)	<(DHA)	<i>d</i> (D⋯A)	A
N4–H41	0.89(2)	2.21(2)	158(2)	3.055(2)	O11T ^a
N4–H41	0.89(2)	2.61(3)	137(2)	3.32(1)	O11U ^a
N4–H41	0.89(2)	2.30(3)	148(2)	3.10(1)	O12U ^a
N11–H111	0.89(2)	1.94(2)	165(2)	2.813(1)	O12T ^a
N11–H111	0.89(2)	2.01(2)	155(2)	2.85(1)	O12U ^a
O32–H32O	0.78(2)	1.79(3)	177(3)	2.573(1)	O22 [–x+1, –y, –z+1]

^a Oxygen atoms of disordered trifluoroacetate anion: label “T” was used for the more abundant position (88%), label “U” for the less abundant position (12%).

Table S13. Experimental data of crystal structures.

	H ₂ L	(H ₄ L)(ClO ₄) ₂	<i>trans</i> -[Cu(L)]· 2CH ₃ OH (III^A)	<i>trans</i> -[Cu(L)]· 2H ₂ O (III^B)	<i>trans</i> -[Cu(H ₂ L)]Cl ₂ (III^C)	<i>trans</i> -[Cu(HL)]Cl· H ₂ O (III^D)	<i>trans</i> -[Cu(H ₂ L)] (CF ₃ CO ₂) ₂ (III^E)	<i>trans</i> -[Cu(H ₂ L)] [Cu(H ₂ L)(SO ₄) ₂]· 6CH ₃ OH (III^F)	<i>cis</i> -[Cu(HL)] ₂ SO ₄ · 6CH ₃ OH (V^A)	<i>cis</i> -[Cu(HL)] (CF ₃ CO ₂) (V^B)
Empirical formula	C ₂₄ H ₃₆ N ₄ O ₂	C ₂₄ H ₃₈ Cl ₂ N ₄ O ₁₀	C ₂₆ H ₄₂ CuN ₄ O ₄	C ₂₄ H ₃₈ CuN ₄ O ₄	C ₂₄ H ₃₆ Cl ₂ CuN ₄ O ₂	C ₂₄ H ₃₇ ClCuN ₄ O ₃	C ₂₈ H ₃₆ CuF ₆ N ₄ O ₆	C ₂₇ H ₄₈ CuN ₄ O ₉ S	C ₅₄ H ₉₄ Cu ₂ N ₈ O ₁₄ S	C ₂₆ H ₃₅ CuF ₃ N ₄ O ₄
Formula weight	412.57	613.48	538.17	510.12	547.01	528.56	702.15	668.29	1238.51	588.12
Crystal system	Monoclinic	Monoclinic	Triclinic	Monoclinic	Monoclinic	Monoclinic	Monoclinic	Monoclinic	Triclinic	Monoclinic
Space group	P 21/n	P 21/c	P -1	P 21/c	P 21/c	P 21/c	P 21/c	P 21/c	P -1	P 21/c
<i>a</i> , Å	8.3779(7)	9.9895(4)	8.8895(3)	9.1079(6)	9.4953(3)	9.3594(4)	10.2817(5)	11.1466(7)	10.4470(9)	8.2800(3)
<i>b</i> , Å	10.8436(9)	16.3405(7)	10.6168(3)	7.9972(5)	8.1407(3)	8.0453(3)	14.9160(6)	15.5923(7)	17.1641(15)	17.1762(8)
<i>c</i> , Å	12.1950(11)	9.0169(4)	14.1906(4)	16.0972(9)	16.1750(6)	16.0783(6)	9.8782(5)	17.9463(10)	19.1368(17)	18.4257(9)
α, °	90	90	100.0640(10)	90	90	90	90	90	64.427(3)	90
β, °	94.231(2)	110.7870(10)	105.3310(10)	95.474(2)	97.589(1)	96.7660(10)	103.850(2)	93.646(2)	89.789(3)	94.991(2)
γ, °	90	90	90.9600(10)	90	90	90	90	90	74.342(3)	90
Volume, Å ³	1104.86(16)	1376.05(10)	1268.95(7)	1167.14(12)	1239.35(8)	1202.25(8)	1470.89(12)	3112.8(3)	2955.2(5)	2610.5(2)
Z	2	2	2	2	2	2	2	4	2	4
Reflections collected	10963	16894	30874	11463	12144	15693	53159	35816	139754	41223
Independent reflections	2146	3154	5808	2654	2441	2753	3369	7130	13536	5986
	[<i>R</i> (int) = 0.0231]	[<i>R</i> (int) = 0.0181]	[<i>R</i> (int) = 0.0267]	[<i>R</i> (int) = 0.0372]	[<i>R</i> (int) = 0.0370]	[<i>R</i> (int) = 0.0175]	[<i>R</i> (int) = 0.0293]	[<i>R</i> (int) = 0.0573]	[<i>R</i> (int) = 0.0381]	[<i>R</i> (int) = 0.0343]
Data / restraints / parameters	2146 / 0 / 144	3154 / 0 / 193	5808 / 0 / 337	2654 / 0 / 163	2441 / 0 / 159	2753 / 0 / 164	3369 / 55 / 266	7130 / 0 / 405	13536 / 0 / 785	5986 / 12 / 390
Final <i>R</i> indices	<i>R</i> ₁ = 0.0348	<i>R</i> ₁ = 0.0297	<i>R</i> ₁ = 0.0284,	<i>R</i> ₁ = 0.0555,	<i>R</i> ₁ = 0.0300,	<i>R</i> ₁ = 0.0270,	<i>R</i> ₁ = 0.0293,	<i>R</i> ₁ = 0.0390,	<i>R</i> ₁ = 0.0596,	<i>R</i> ₁ = 0.0270,
[<i>I</i> > 2σ(<i>I</i>)]	<i>wR</i> ₁ = 0.0858	<i>wR</i> ₁ = 0.0800	<i>wR</i> ₁ = 0.0731	<i>wR</i> ₁ = 0.1427	<i>wR</i> ₁ = 0.0765	<i>wR</i> ₁ = 0.0687	<i>wR</i> ₁ = 0.0782	<i>wR</i> ₁ = 0.0857	<i>wR</i> ₁ = 0.1698	<i>wR</i> ₁ = 0.0696
<i>R</i> indices (all data)	<i>R</i> ₂ = 0.0356	<i>R</i> ₂ = 0.0318	<i>R</i> ₂ = 0.0317,	<i>R</i> ₂ = 0.0593,	<i>R</i> ₂ = 0.0345,	<i>R</i> ₂ = 0.0275,	<i>R</i> ₂ = 0.0299,	<i>R</i> ₂ = 0.0513,	<i>R</i> ₂ = 0.0676,	<i>R</i> ₂ = 0.0292,
	<i>wR</i> ₂ = 0.0864	<i>wR</i> ₂ = 0.0814	<i>wR</i> ₂ = 0.0750	<i>wR</i> ₂ = 0.1448	<i>wR</i> ₂ = 0.0794	<i>wR</i> ₂ = 0.0690	<i>wR</i> ₂ = 0.0787	<i>wR</i> ₂ = 0.0909	<i>wR</i> ₂ = 0.1795	<i>wR</i> ₂ = 0.0709
CCDC number	2392220	2392217	2392214	2392215	2392211	2392213	2392216	2392212	2392219	2392218

Theoretical calculations

Relative energies of isomers in the model using a purely implicit solvent

One of the features of implicit solvent model used in calculations in **Table S14** is that while the internal hydrogen bonds are described explicitly, the possible hydrogen bonds with solvent molecules are only covered by implicit solvent model. An ideal accurate model would consider a full inclusion of the first solvation shell in simulations, which is however an expensive approach. The core of the problem lies in the fact that in the case of our complexes the strength of the coordination bond of the protonated phenolate is comparable to both intramolecular hydrogen bonds and hydrogen bonds within the aqueous solvent.

According to the experimental data, the most common isomer of cyclam complexes is *trans-III*. In the calculations with the purely implicit solvent, in the diprotonated form, $[\text{Cu}(\text{H}_2\text{L})]^{2+}$, the *trans-III* is calculated to be clearly the most stable isomer, with *cis-I* and *trans-II* isomers lying 4–5 kcal/mol higher. However, in the monoprotinated form, the *trans-III*, *cis-I* and *cis-V* isomers all have comparable energies with the *cis-I* isomer being the lowest one. In the fully protonated form, *trans-III* is the lowest isomer with the closest lying *trans-II* isomer 4.6 kcal/mol higher. The lowest-energy minimum structures were obtained by generating series of possible conformers and subsequent DFT minimizations using implicit solvent model (see Methods). The obtained lowest energy minima are plotted in **Figures S11-S13**. The predicted relative energies are listed in **Table S14**.

The energy of the monoprotinated *cis-I* and *cis-V* isomers appears unexpectedly low in **Table S14**, because experimental data showed that the *trans-III* is the lowest isomer, because it is the thermodynamic product formed after heating regardless pH. It indicates that the reverse energy order results from the formation of the intramolecular hydrogen bonds between the protonated and deprotonated phenolate pendant arms (**Figure S12**). The internal hydrogen bonds in the calculated structures also contrast with the X-ray structures of *cis-V* isomer (**Figure 6**), where the protonated pendant arm actually forms hydrogen bonds outside the center of the complex. In addition, the strong calculated intramolecular bond results in unrealistically high value of the corresponding protonation constant in the *cis*-isomers (**Table 16**).

The effect of the explicit water molecules is illustrated on bonding distances between copper and phenolate oxygen atom (**Table S17**). In the crystals of the *cis-V* isomer the Cu–O bond is rather short, at 1.97 Å, that is 0.06–0.09 Å shorter than the Cu–O distances calculated in solvent. This can be rationalized by fact that in crystal, there are no *intramolecular* hydrogen bonds between the pendant arms and one phenolate is uncoordinated and involved in *intermolecular* hydrogen bonding. The situation is different in solution, where calculations

propose, that intramolecular hydrogen bonding leads to the lengthening of the coordination Cu–O bond. In the *cis-I* and *cis-V* monoprotonated systems in solution, the intramolecular hydrogen bonding causes extension of the Cu–O bond of the bonded phenolate to 2.20 and 2.03 Å, respectively. Inclusion of explicit waters leads to further elongation of Cu–O bond to 2.33 and 2.06 Å in the *cis-I* and *cis-V* monoprotonated systems. Such elongation is connected to weakening of the coordination bond, that is confirmed in the calculated decrease of the delocalization index for Cu–O bonding in **Table S17**. The difference between results obtained for both models (with and without explicit water molecules) points out to the increase of the relative energy of the monoprotonated *cis-I* and *cis-V* isomers, that is inherently linked to the reduction of the overstabilizing effect of the intramolecular hydrogen bonds in these isomers. We note that even with explicit solvent the intramolecular hydrogen bonds remain at place while correct energetics is obtained.

Table S14. Predicted relative electronic energies^a of the lowest minima of isomers relative to the isomer **III** in the purely implicit solvent. For structures, see **Figures S11-S13**.

Isomer	Relative energy [kcal/mol]		
	[Cu(H ₂ L)] ²⁺	[Cu(HL)] ⁺	[Cu(L)]
<i>cis-I</i>	4.1	-1.3	10.8
<i>trans-II</i>	5.0	3.9	4.6
<i>cis-II</i>	9.5	5.7	12.6
<i>trans-III</i>	0.0	0.0	0.0
<i>trans-IV</i>	11.4	11.4	11.0
<i>cis-V</i>	13.2	2.2	10.9

^a Relative to *trans-III* isomer for each of the protonated states. Calculated at DFT BP86-D3BJ/def2TZVP/PCM ($\epsilon = 80$) level, see Methods.

Table S15. Predicted relative electronic energies^a of the lowest minima of isomers relative to the isomer **III** in the model with two explicit water molecules included. For structures, see **Figures 7, S14 and S15**.

Isomer	Relative energy [kcal/mol]		
	[Cu(H ₂ L)] ²⁺ +	[Cu(HL)] ⁺	[Cu(L)]
<i>cis-I</i>	6.1	3.1	8.5
<i>trans-II</i>	5.0	5.6	4.9
<i>cis-II</i>	12.2	5.2	8.7
<i>trans-III</i>	0.0	0.0	0.0
<i>trans-IV</i>	11.8	12.2	11.5
<i>cis-V</i>	7.3	5.1	12.0

^a Relative to *trans-III* isomer for each of the protonated states. Calculated at DFT BP86-D3BJ/def2TZVP/PCM ($\epsilon = 80$) level, see Methods.

Table S16. Calculated protonation constants pK_A^a of individual isomers in the models with the purely implicit solvent and with the two explicit water molecules included.

Isomer	Purely implicit solvent		Two explicit water molecules	
	pK_{HL}	pK_{H2L}	pK_{HL}	pK_{H2L}
<i>cis-I</i>	13.3	6.64	9.33	6.83
<i>cis-II</i>	11.5	4.95	10.2	6.72
<i>trans-II</i>	8.97	6.17	8.97	8.30
<i>trans-III</i>	7.50	7.17	8.10	8.03
<i>trans-IV</i>	10.6	7.36	8.70	7.11
<i>cis-V</i>	10.0	8.80	9.09	6.35

^a The individual changes in the Gibbs free energy for all isomers in deprotonated, monoprotinated, and diprotinated forms are provided in **Tables 1 and S20**. For computational protocol, see Methods.

Table S17. Predicted^a interatomic O-O/M distances and calculated delocalization indices for selected bonds and isomers.

Isomer		Cu-O [Å]	DI _{Cu-O}
<i>cis-I</i>	Implicit solvent	2.20	0.29
	Two explicit water molecules	2.33	0.27
<i>cis-V</i>	Implicit solvent	2.03	0.40
	Two explicit water molecules	2.06	0.41
	Experimental data from X-ray	1.97 ^b	0.41

^a Geometries at BP86-D3/def2-TZVP(PCM) level, see Methods.

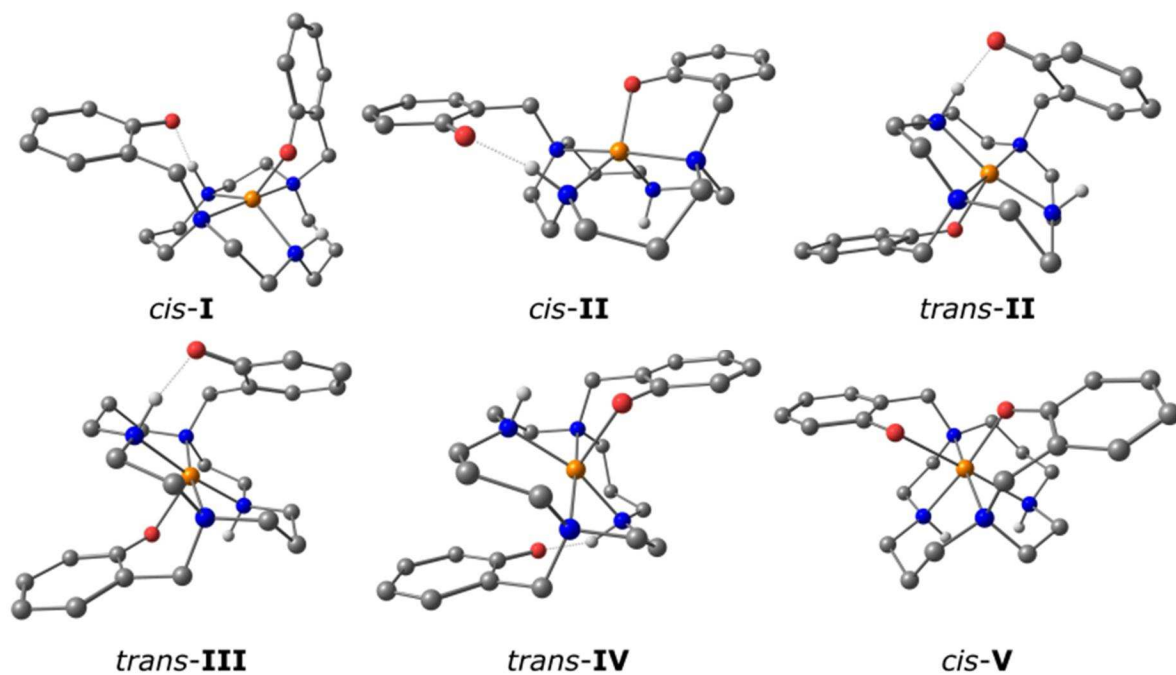


Figure S11. Calculated optimized structures of deprotonated isomers. For relative electronic energies, see **Table S14**. For COSMO-RS relative ΔG energies, see **Table S20**.

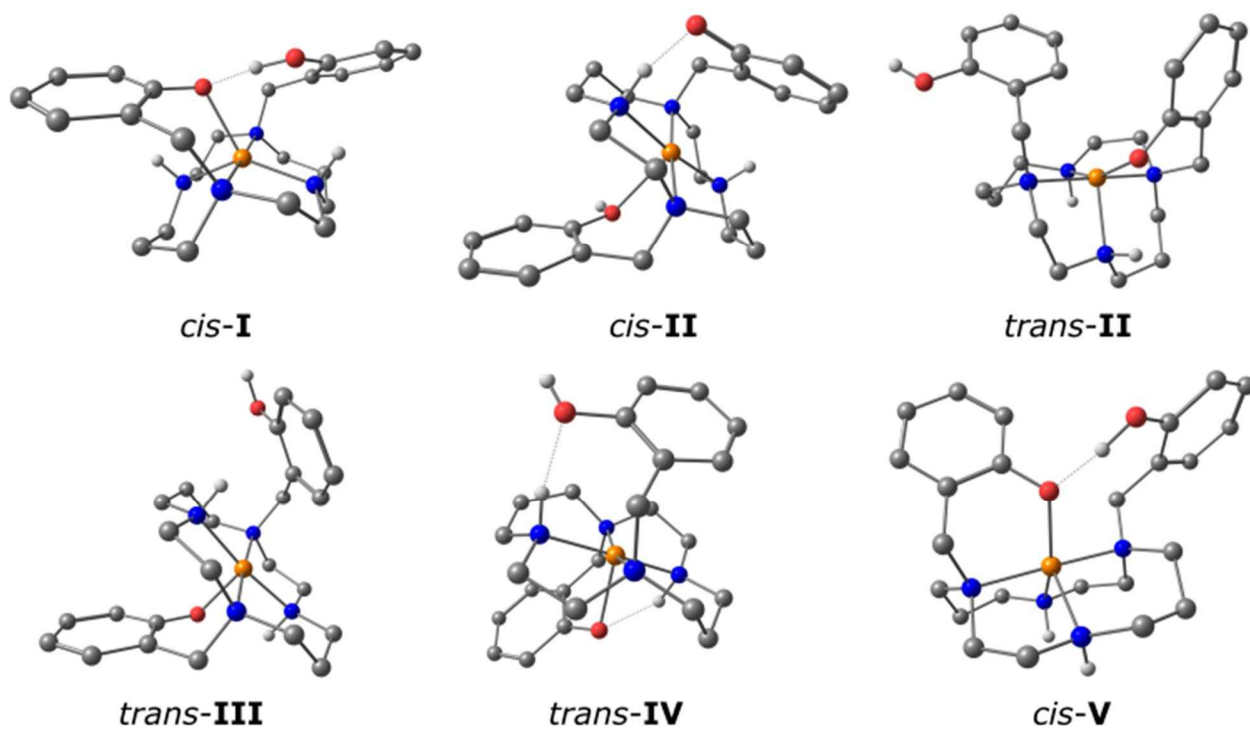


Figure S12. Calculated optimized structures of monoprotinated isomers. For relative electronic energies, see **Table S14**. For COSMO-RS relative ΔG energies, see **Table S20**.

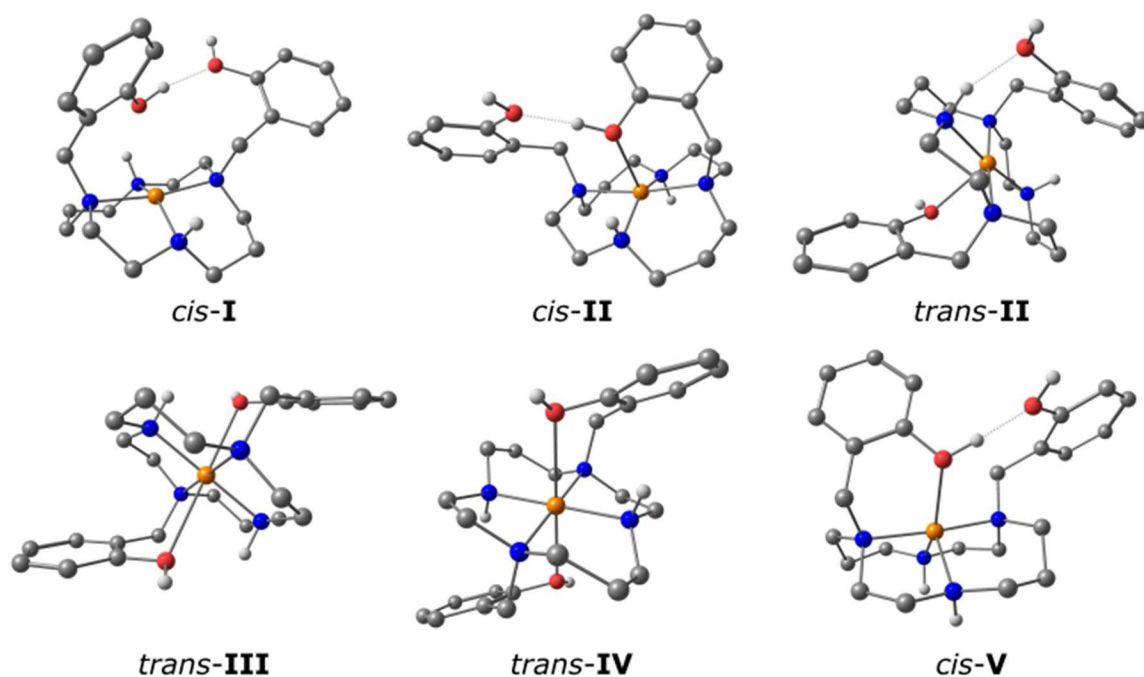


Figure S13. Calculated optimized structures of diprotonated isomers. For relative electronic energies, see **Table S14**. For COSMO-RS relative ΔG energies, see **Table S20**.

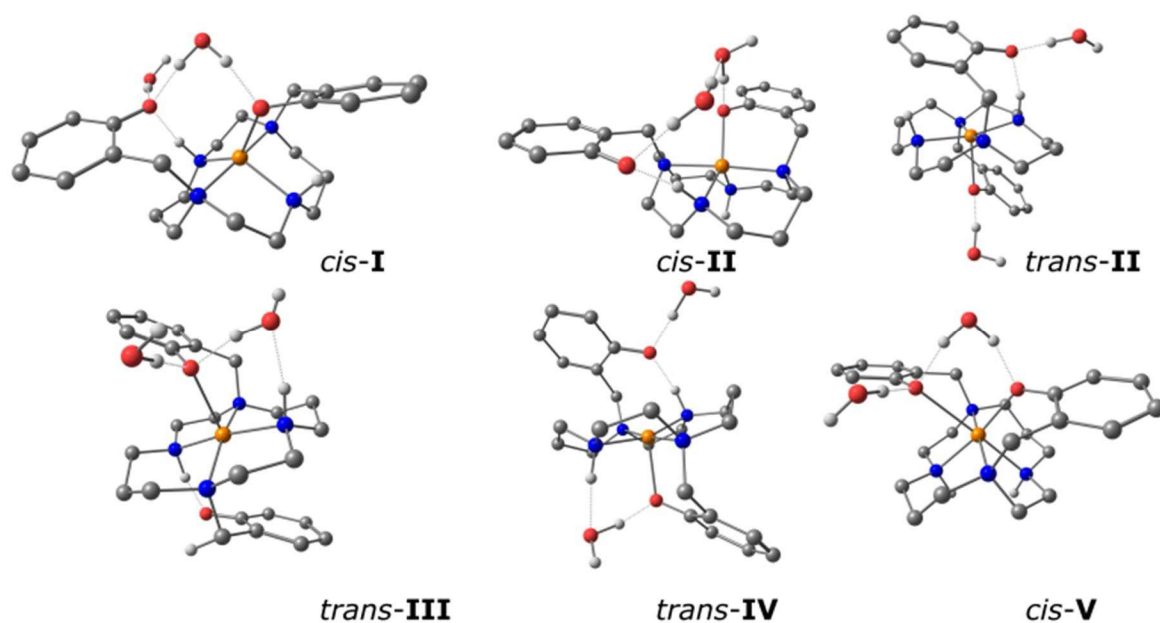


Figure S14. Optimized structures of deprotonated isomers calculated in the model with the two explicit water molecules included. For relative electronic energies, see **Table S15**. For COSMO-RS relative ΔG energies, see **Table 1**.

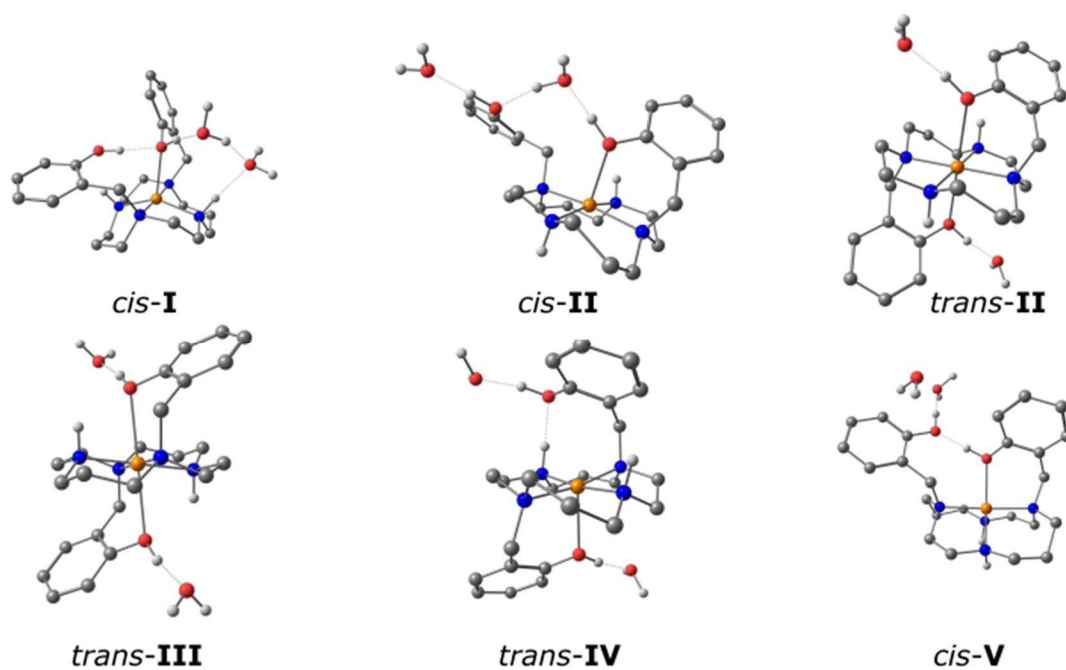


Figure S15. Optimized structures of diprotonated isomers calculated in the model with the two explicit water molecules included. For relative electronic energies, see **Table S15**. For COSMO-RS relative ΔG energies, see **Table 1**.

Table S18. Calculated reduction potentials of deprotonated, monoprotonated and diprotonated isomers based on the model with purely implicit solvent or with two explicit water molecules.

Isomer	Calculated potentials E [V]					
	Purely implicit solvent			Two explicit water molecules		
	[Cu(H ₂ L)] 2+	[Cu(HL)] ⁺	[CuL]	[Cu(H ₂ L)] 2+	[Cu(HL)] ⁺	[CuL]
<i>cis-I</i>	-0.34	-0.66	-0.79	-0.22	-0.61	-0.67
<i>cis-II</i>	-0.23	-0.40	-0.48	-0.24	-0.25	-0.50
<i>trans-II</i>	-0.18	-0.42	-0.54	-0.24	-0.34	-0.48
<i>trans-III</i>	-0.33	-0.51	-0.88	-0.34	-0.52	-0.72
<i>trans-IV</i>	-0.17	-0.26	-0.42	-0.13	-0.19	-0.41
<i>cis-V</i>	-0.28	-0.62	-0.68	-0.31	-0.57	-0.59

Table S19. Predicted^a interatomic M-O/N distances in the lowest conformers in the model with two explicit water molecules.

Isomer	[Cu(H ₂ L)] ²⁺		[Cu(HL)] ⁺		[CuL]	
	Cu-OH	Cu-OH	Cu-O ⁻	Cu-OH	Cu-O ⁻	Cu-O ⁻
<i>cis-I</i>	2.352	3.334	2.329	2.970	2.141	3.318
<i>trans-II</i>	2.427	3.525	2.304	5.097	2.248	3.487
<i>cis-II</i>	2.405	4.841	2.161	4.309	2.074	4.133
<i>trans-III</i>	2.593	2.604	2.328	4.977	2.336	3.398
<i>trans-IV</i>	2.592	2.596	2.330	3.739	2.279	3.022
<i>cis-V</i>	2.243	4.167	2.058	4.131	2.021	2.628

^a Geometries at BP86-D3/def2-TZVP(PCM) level, see Methods.

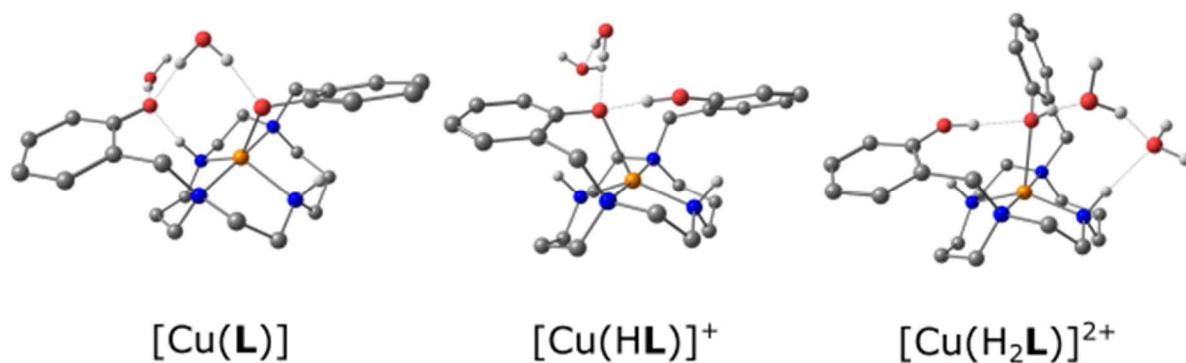


Figure S16. Calculated optimized structures of the *cis-I* isomer in all studied protonation states with two explicit water molecules. For relative ΔG energies, see Table 1. For bond distances, see Table 3.

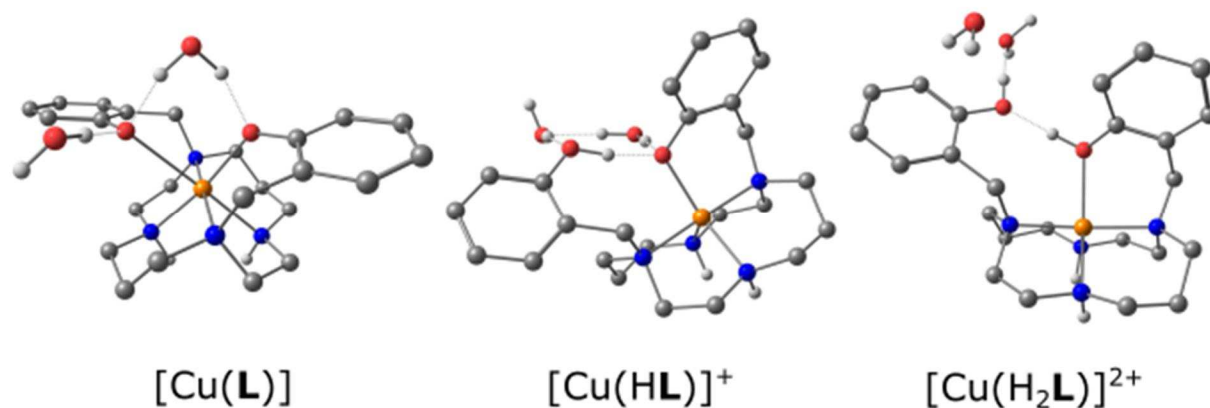


Figure S17. Calculated optimized structures of the *cis-V* isomer in all studied protonation states with two explicit water molecules. For relative ΔG energies, see Table 1. For bond distances, see Table 3.

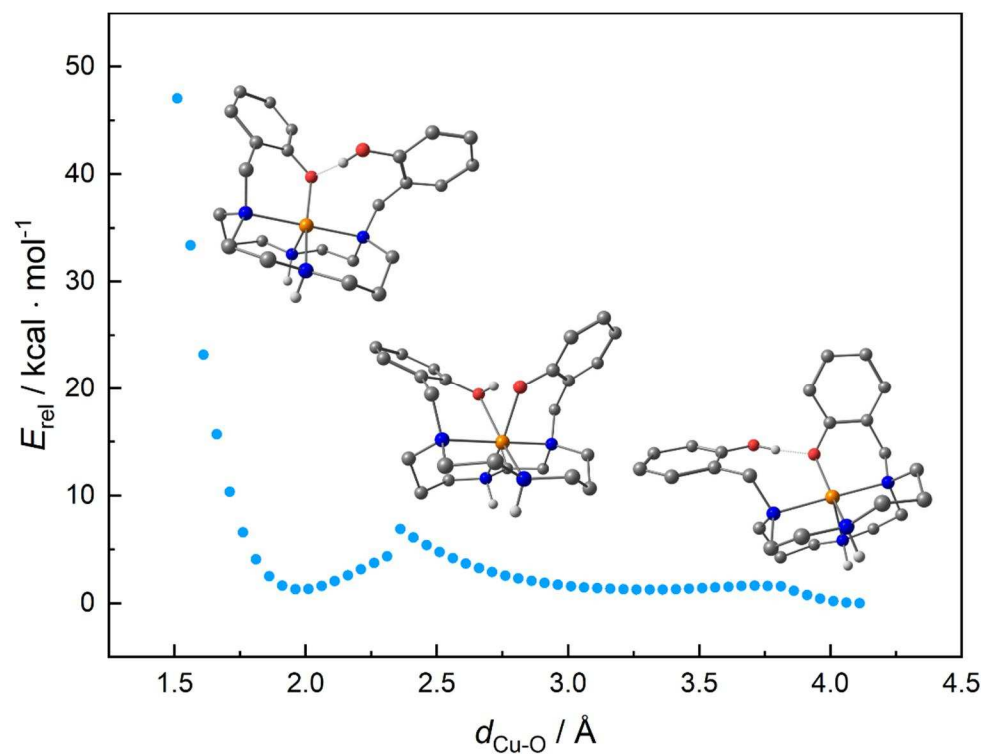


Figure S18. Energy scan as function of Cu–O distance in the monoprotonated isomer *cis-V*.

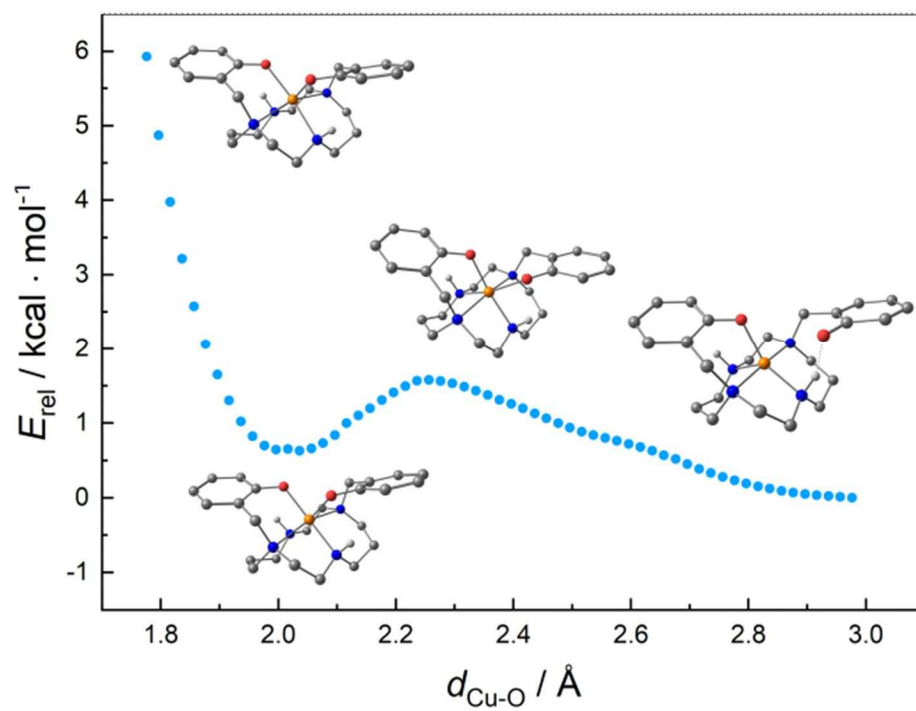


Figure S19. Energy scan as function of Cu–O distance in the deprotonated isomer *cis-I*.

Table S20. Predicted relative total free Gibbs energies from the COSMO-RS protocol of the lowest [Cu(L)] conformers relative to the isomer *trans-III*.

Isomer	Relative energy [kcal/mol]		
	[Cu(H ₂ L)] ²⁺	[Cu(HL)] ⁺	[Cu(L)]
<i>cis-I</i>	11.68	3.78	6.73
<i>cis-II</i>	12.94	7.53	12.69
<i>trans-II</i>	5.38	3.44	6.92
<i>trans-III</i>	0.00	0.00	0.00
<i>trans-IV</i>	15.18	10.98	12.84
<i>cis-V</i>	7.98	4.62	15.46